Invisible Bias: Amorphous Silica Cement as a Source of Petrophysical Non-Reproducibility

Matthias Halisch[1,*], and *Marina* Dercks[1]

[1]LIAG-Institute for Applied Geophysics, Dept. F2.2 Petrophysical Characterization, Stilleweg 2, D-30655 Hanover, Germany

Abstract. Reproducibility is a fundamental requirement in core analysis and forms the basis for inter-laboratory comparability, workflow validation, and petrophysical model calibration. Quartz-rich reference sandstones such as Fontainebleau are commonly assumed to provide stable and reproducible laboratory responses because of their simple mineralogy and high purity. However, repetitive measurements on selected Fontainebleau specimens revealed unexpected variability in interface-sensitive petrophysical data. Nuclear magnetic resonance measurements showed pronounced shifts in transverse relaxation time distributions, while total porosity remained nearly constant. In parallel, spectral induced polarization measurements exhibited strong variations in phase response and imaginary conductivity, whereas direct-current resistivity was largely unaffected. Conventional mineralogical analyses did not indicate swelling clays or other highly reactive phases. A consistent pattern emerged only through repeated measurements, controlled conditioning, and cross-method comparison. Scanning electron microscopy of freshly fractured surfaces revealed localized intergranular SiO_2 films with a fractured, wallpaper-like texture, interpreted as amorphous silica cement. Selective leaching experiments stabilized the nuclear magnetic resonance and spectral induced polarization responses, confirming the controlling role of this mineral phase. The results demonstrate that subtle hydration-sensitive silica cements may introduce systematic measurement bias even in well-established reference rocks. The study highlights the importance of conditioning control, repeated measurements, and integrated petrophysical workflows for identifying hidden sources of non-reproducibility in laboratory core analysis.

1 Introduction

Core-analysis and SCAL demand highly reproducible samples with known mineralogy and fluid history. Pure quartz sandstones (e.g. Fontainebleau Formation, Paris Basin) are treated as reference media because of their simple composition. Yet recent observations show that even “pure” sandstones may contain fine amorphous silica coatings or cements that escape standard detection, introducing an “invisible bias” in petrophysical data. In Fontainebleau sandstone, repeated NMR and SIP tests varied unpredictably until it was found that hydration-sensitive amorphous SiO_2 films control pore-water relaxation and polarization responses. This motivates a review of how amorphous silica cements form in sandstones. We outline the sources and diagenetic pathways of amorphous SiO_2, the environmental controls (e.g., pH, ionic strength, organic ligands), their characteristic micro-textures, and how they ultimately transform to quartz. Understanding these processes helps detect hidden silica phases and explains anomalies in porosity and potentially in geophysical log interpretation.

1.1 Amorphous Silica in Quartz-Rich Sandstones

Amorphous and poorly ordered silica phases represent metastable forms of SiO_2 that precipitate within the pore space of sedimentary rocks under low-temperature diagenetic conditions [1–5]. Unlike crystalline quartz, they lack long-range lattice order and commonly occur as silica gels, nanometer-scale films, colloidal aggregates, opaline cements, or cryptocrystalline precursor phases [1,3]. In sandstone systems, they are typically associated with opal-A, opal-CT, chalcedony-like silica, and microcrystalline quartz formed during progressive recrystallization [1,5]. Although volumetrically minor, these phases may exert a disproportionate influence on pore-surface properties because they preferentially occur as grain-coating or pore-lining cements rather than massive pore-filling quartz [2–4].

Amorphous silica precipitates whenever dissolved silica exceeds its local solubility within the pore-fluid system [5]. Silica may be supplied by weathering and dissolution of feldspars or clay minerals, biogenic silica, volcanic glass alteration, or groundwater-driven silicification processes [1,2,5]. In quartz-rich systems such as the Fontainebleau Formation, precipitation has been linked to hydrologically controlled groundwater processes involving fluid mixing, cooling, evaporation, or changes in pH and ionic strength [2–4]. Under these conditions, metastable silica may initially form gels or poorly ordered films before recrystallizing into microquartz or syntaxial quartz overgrowths [2–4].

* Corresponding author: matthias.halisch@liag-institut.de

The transformation from amorphous silica to crystalline quartz generally follows the sequence opal-A → opal-CT → microcrystalline quartz → quartz [1,5]. Although controlled by temperature, time, fluid chemistry, and surface conditions, poorly ordered silica may persist over geological timescales under shallow-burial conditions where crystallization kinetics remain inhibited [2,5]. Cathodoluminescence, scanning electron microscopy (SEM), electron backscatter diffraction (EBSD), and neutron pair-distribution-function studies indicate that Fontainebleau sandstone experienced at least part of its cementation history through metastable amorphous or poorly ordered silica precursor phases that subsequently recrystallized into quartz or microquartz coatings [1–4].

Such phases are difficult to identify using conventional bulk mineralogical methods. X-ray diffraction generally records only broad amorphous humps or weak opal-CT reflections, whereas X-ray fluorescence merely reports total SiO_2 without distinguishing silica polymorphs or hydration states [1,4]. Reliable identification therefore requires microstructural and interface-sensitive techniques such as SEM, cathodoluminescence, transmission electron microscopy, Raman spectroscopy, or electron microprobe analysis [1–4]. Characteristic textures include isopachous rims, globular or botryoidal silica aggregates, nanometer-scale intergranular films, and fractured "wallpaper-like" coatings on fresh fracture surfaces (Fig. 1) [1–4].

Because amorphous silica is structurally disordered, hydrated, and rich in silanol-bearing surface sites, its physical and electrochemical properties differ markedly from those of crystalline quartz [5]. Even thin silica films may therefore modify pore-surface relaxation, fluid-mineral interactions, interfacial electrical polarization, and micropore accessibility without measurably changing bulk mineralogy or total porosity [1,3,4]. Their occurrence in otherwise quartz-dominated reference sandstones is therefore highly relevant for interface-sensitive petrophysical methods and laboratory reproducibility.

1.2 Motivation for this Work

The present study originated from repeated combined nuclear magnetic resonance and spectral induced polarization measurements performed on Fontainebleau sandstone samples during multiple saturation–measurement–drying cycles using the same electrolyte and identical laboratory procedures. Despite careful conditioning and stable bulk petrophysical parameters, the measurements showed persistent non-reproducibility. The variability was particularly pronounced in the short transverse relaxation time components of the nuclear magnetic resonance response and in the medium- to low-frequency range of the spectral induced polarization spectra, whereas total porosity and direct-current resistivity remained comparatively stable.

Initially, instrumental instability, electrode effects, saturation artifacts, and processing errors were considered as possible explanations. However, repeated calibration tests, cross-checks between instruments, and systematic repetition of the measurements progressively excluded experimental malfunction as the primary cause. The reproducibility problem instead appeared to be linked to the rock material itself and to subtle changes occurring during repeated hydration and drying cycles.

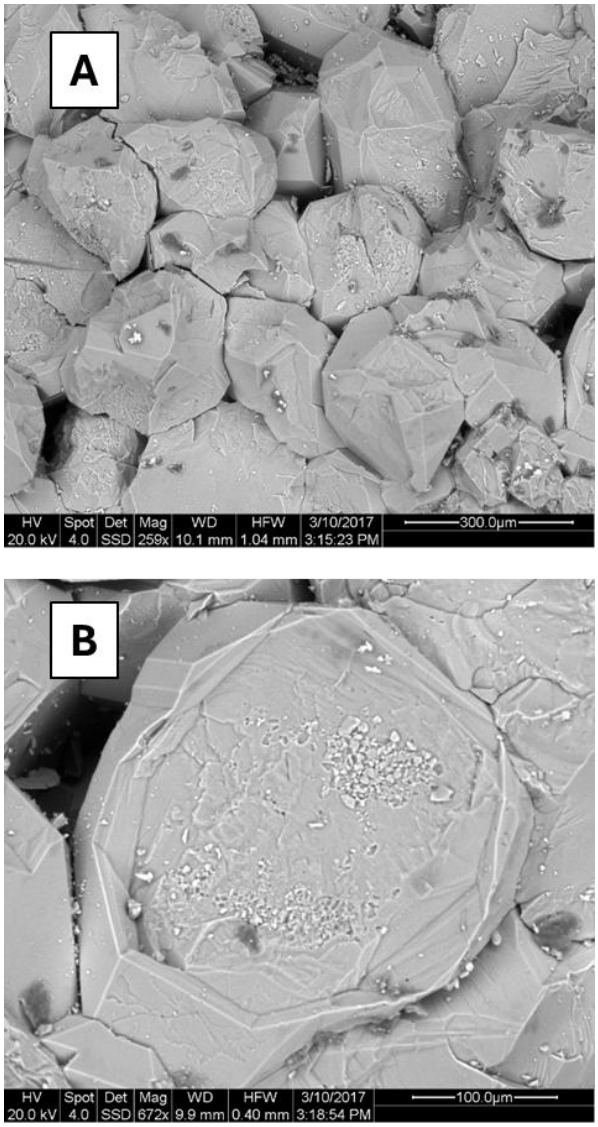

Figure 1: "Wallpaper" like structures as visual evidence for amorphous silica cement in Fontainebleau Sandstone, imaged by SEM. (A) showcases an overview, (B) a close-up of the "wallpaper" like structures that remain at former grain-grain contact zones.

This observation triggered a detailed re-evaluation of the supposedly simple quartz-dominated reference sandstone. Subsequent microscopic and mineralogical investigations revealed localized intergranular SiO_2 films with characteristic fractured textures that were largely invisible in conventional bulk mineralogical screening. Their morphology, spatial occurrence, and hydration-sensitive behavior suggested the presence of amorphous or poorly ordered silica phases capable of modifying pore-scale surface relaxation and interfacial electrical

polarization without substantially affecting bulk porosity or mineralogy.

Although amorphous silica has repeatedly been described from Fontainebleau sandstone, its influence on the reproducibility of interface-sensitive laboratory measurements has, to the authors' knowledge, not yet been systematically investigated. The present study addresses this gap by combining repeated NMR and SIP measurements with selective alkaline leaching and microstructural characterization.

2 Impact on CAL and SCAL

Amorphous and poorly ordered silica phases are commonly regarded as minor diagenetic components in quartz-rich reservoir rocks. However, their influence on routine core analysis (CAL) and special core analysis (SCAL) may be disproportionate to their volumetric abundance [1,3,4,6]. These phases include opal-A, opal-CT, poorly crystalline silica, gel-like SiO_2, and thin amorphous or cryptocrystalline precursor films that may later recrystallize into chalcedony, microquartz, or macrocrystalline quartz [1,3,4,6]. From a petrophysical perspective, the morphology, crystallinity, surface state, and paragenetic position of the cement are more important than its overall abundance. While pore-filling silica may reduce porosity and permeability, thin pore-lining films can preserve intergranular porosity by inhibiting syntaxial quartz overgrowth while simultaneously increasing surface-controlled microporosity [1,3,4].

Direct CAL/SCAL impacts have been reported particularly for diatomitic and opal-CT-bearing systems. Imbibition studies demonstrated that highly siliceous fine-grained rocks may exhibit strong capillary uptake despite extremely low permeability, while counter-current imbibition and relative-permeability estimates are affected by pronounced non-equilibrium effects [7,8]. High-temperature SCAL experiments further documented changes in wettability, endpoint saturations, pore-size distributions, and silica phase transformations during thermal-fluid exposure [9–12]. These studies demonstrate that the pore system and mineral surfaces may evolve during the experiment itself rather than remaining static.

Comparable observations have been reported for silica-bearing chalk reservoirs, where permeability, capillary entry pressure, wettability, and spontaneous imbibition are controlled not only by porosity but also by specific surface area and silica-rich surface phases [13,14]. Even relatively small amounts of silica-rich cement may therefore significantly influence SCAL-derived parameters.

For quartz-rich sandstones, the effects are more subtle but potentially equally important. Studies of the Fontainebleau Sandstone demonstrate that this widely used reference rock is not mineralogically trivial. Neutron pair-distribution-function analysis suggested the presence of a glass-like amorphous silica component despite quartz-dominated bulk mineralogy [6], while cathodoluminescence, SEM, EBSD, and TEM revealed heterogeneous cement zones, poorly ordered silica, amorphous nanofilms, and misoriented microquartz coatings [1–4]. Nanometer-scale amorphous silica films can isolate detrital quartz grains from later syntaxial overgrowth, thereby either preserving porosity through non-epitaxial cementation or reducing permeability by partial pore filling [3,4]. Consequently, the petrophysical impact depends primarily on cement morphology and surface distribution rather than on bulk silica content.

This distinction is particularly relevant because amorphous silica influences both geometry-sensitive and interface-sensitive petrophysical methods. Besides modifying pore-throat geometry and capillary behavior, silanol-rich amorphous silica surfaces alter surface relaxivity, proton exchange, electrical double-layer properties, and interfacial polarization without substantially changing bulk mineralogy or total porosity [3,4,15,16]. Fontainebleau-specific NMR studies identified multiple relaxation populations associated with intergranular pores and coating-related microporosity [15], while electrical investigations demonstrated measurable surface conductivity even in clay-poor samples [16]. These observations suggest that hydration-sensitive amorphous silica films may generate significant variability in NMR and SIP responses while leaving DC resistivity largely unaffected (Figure 2).

The present study addresses this gap between existing diagenetic observations and petrophysical laboratory practice. Repeated measurements on Fontainebleau specimens revealed unstable NMR relaxation-time distributions and SIP phase responses despite stable bulk porosity and DC resistivity. XRD and XRF excluded swelling clays and other highly reactive mineral phases, whereas SEM and electron microprobe analyses identified localized intergranular amorphous SiO_2 films. Subsequent selective leaching stabilized both NMR and SIP responses, indicating that thin hydration-sensitive silica films may represent previously overlooked interface-active phases capable of systematically biasing laboratory core-analysis measurements.

From a CAL/SCAL perspective, several practical implications emerge. Amorphous silica should be considered during the screening and interpretation of reference rocks and reservoir analogues, and petrophysical classification should include silica phase, cement morphology, and surface characteristics in addition to conventional bulk mineralogy and porosity-permeability relationships. Furthermore, chemically reactive or long-duration laboratory experiments may alter metastable silica phases during testing. Repeated measurements and standardized conditioning should therefore be regarded not only as quality-control procedures but also as diagnostic tools for identifying hidden surface-active phases and non-reproducible petrophysical behavior.

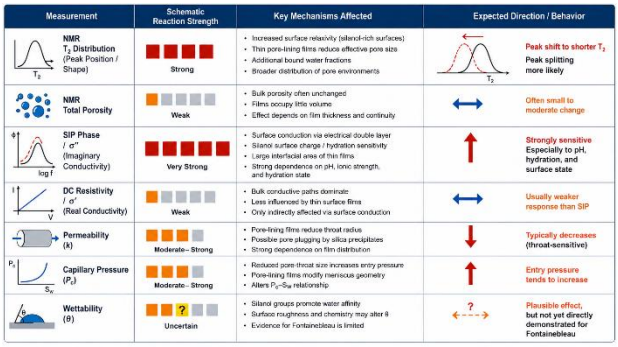

Figure 2: Qualitative impact of amorphous silica on petrophysical measurements as observed by [6-15].

3 Fontainebleau Sample Material

The present study uses Fontainebleau Sandstone as a reference material for investigating hidden diagenetic controls on petrophysical reproducibility. Owing to its exceptionally high quartz purity, the sandstone is widely used for calibration experiments, laboratory benchmarking, petrophysical method comparison, and fundamental pore-scale studies. Its apparent mineralogical simplicity makes it particularly suitable for assessing whether subtle hydration-sensitive phases can introduce measurable variability in routine core analysis (CAL) and special core analysis (SCAL). If such effects occur even in this quartz-dominated reference sandstone, they are likely to be even more pronounced in compositionally more complex reservoir rocks.

Previous petrographic and diagenetic studies demonstrate that the Fontainebleau Sandstone cannot be regarded simply as a framework of detrital quartz grains with syntaxial quartz overgrowths. Instead, its silicification history reflects the interaction of groundwater flow, near-surface to shallow-burial diagenesis, silica mobilization, and metastable silica precipitation [1–4,15,16]. Several authors further proposed that poorly ordered or amorphous silica acted as precursor cement during parts of this diagenetic evolution [17–20]. Consequently, Fontainebleau provides an ideal natural laboratory for investigating whether subtle silica cements influence the reproducibility of interface-sensitive petrophysical measurements.

The investigated material spans different degrees of cementation within the Fontainebleau Formation, allowing strongly cemented, intermediate, and weakly cemented pore fabrics to be compared within the same quartz-dominated mineralogical system. Particular attention is given to the relationship between cement morphology, pore structure, and the reproducibility of nuclear magnetic resonance (NMR) and spectral induced polarization (SIP) measurements.

3.1 Geological and Petrophysical Background

The Fontainebleau Formation occurs in the central Paris Basin and is generally described as a Rupelian to early Oligocene shallow-marine to coastal-aeolian quartz-arenite [2,15,17,18]. The sandstone is typically fine grained, very well sorted, and nearly monomineralic, with the commonly used white Fontainebleau material representing one of the purest quartz-rich end members. Reported petrophysical properties span a large range depending on cementation intensity and stratigraphic position, with porosities ranging from strongly cemented low-porosity domains to values approaching 30% in weakly cemented material, while permeability may vary from a few millidarcies to more than 1 Darcy [15,17]. This combination of mineralogical purity, excellent sorting, and broad petrophysical variability explains why Fontainebleau sandstone is widely used as a calibration and benchmarking material for core-analysis workflows.

The diagenetic evolution of the Fontainebleau Sandstone differs fundamentally from the classical model of deeply buried, temperature-driven quartz cementation. Instead, several studies indicate that silicification occurred predominantly under shallow-burial to near-surface conditions and was closely linked to groundwater circulation, bleaching, leaching, fluctuating paleo-water-table conditions, and hydrologically focused flow paths [2,18-20]. Quartzite lenses and strongly cemented sandstone bodies commonly occur adjacent to weakly cemented or unconsolidated sands, suggesting spatially heterogeneous silicification controlled by groundwater flow rather than uniform burial-related quartz precipitation [2,19]. The literature further described tightly cemented sandstone lenses embedded within otherwise unconsolidated sands and interpreted their formation as a groundwater-controlled silicification process [2]. Their reactive-transport modelling required silica precipitation rates significantly faster than expected for low-temperature quartz growth, supporting the involvement of metastable or poorly ordered silica precursor phases during early cementation [2].

The source and precipitation mechanisms of silica are generally interpreted as a combination of internal silica mobilization and shallow groundwater transport [2,18–20]. Proposed silica sources include weathering and bleaching processes, dissolution of accessory silicate phases, clay-mineral transformation, and dissolution of silica-bearing components within the shallow groundwater system [2,18–20]. Precipitation was likely triggered by changes in temperature, pH, ionic strength, flow regime, or groundwater mixing conditions [2,18–20]. More recent interpretations additionally emphasize the role of glacial to periglacial groundwater circulation and cooling during later silicification stages [19,20]. Although the exact timing of the main silicification event remains debated, the overall consensus is that Fontainebleau records a low-temperature, hydrologically controlled silicification history rather than a simple burial-related quartz-cementation pathway [2,18-20]. The currently discussed silicification mechanisms and their potential relation to amorphous silica formation in the

Fontainebleau Formation are summarized schematically in Table 1.

Several independent studies indicate that at least part of this silica cementation history involved amorphous or poorly ordered precursor phases [1-4,6]. [2] described alternating syntaxial quartz overgrowths and isopachous silica rims interpreted as recrystallized amorphous or poorly ordered silica precursors [2]. [6] identified local structural components consistent with glass-like or amorphous silica despite the quartz-dominated bulk mineralogical signal. SEM, cathodoluminescence, EBSD, and TEM investigations further documented heterogeneous cement textures, micro-quartz coatings, poorly crystalline silica domains, and amorphous nanofilms associated with quartz cement development [1,3,4].

Table 1: Summary of proposed silicification mechanisms in the Fontainebleau Formation and their potential relation to amorphous silica formation.

Mechanism	Inferred Si source	Trigger	typical products	Status for FO
Bleaching, weathering in the profile	flint, clay minerals, accessory phases	supersaturation at discharge zones	SiO2 overgrowths, sharp cementation fronts	well supported
Groundwater cooling	transported Si in the aquifer	frost, permafrost	amorphous/ cryptocrystaline SiO2	strongly supported
Groundwater + recharge mixing	Si-rich groundwater + more acidic seepage water	pH/ionic strength/ complexation change	zoned rim formation	plausible, but unproven
Amorphous nano-films	local supersaturation at grain surfaces	rapid nucleation, inhibited epitaxy	amorphous film, microquartz	strongly supported

[4] demonstrated that microcrystalline quartz in Fontainebleau is not simply a syntaxial continuation of the detrital quartz grains, but may be crystallographically misoriented, consistent with growth on earlier poorly ordered silica surfaces. Comparable work by [3] additionally showed that amorphous silica nanofilms may isolate detrital quartz from later quartz overgrowth and thereby redirect the subsequent cementation pathway.

These observations are directly relevant for petrophysical characterization because the earliest silica cement phase strongly influences the later pore architecture and surface properties of the rock. Whereas syntaxial quartz overgrowths commonly reduce pore-throat radii and permeability, amorphous or chalcedony-like precursor films may inhibit epitaxial quartz growth and promote micro-quartz coatings that partly preserve intergranular porosity [3,4]. Consequently, two Fontainebleau samples with similar bulk quartz contents and comparable helium porosity may nevertheless differ substantially in pore-throat geometry, surface-to-volume ratio, microporosity distribution, surface relaxivity, and interfacial electrical behavior.

Previous petrophysical studies support this interpretation. NMR investigations identified multiple transverse relaxation-time components associated with intergranular macropores and coating-related microporosity in micro-quartz bearing Fontainebleau samples [15]. Short relaxation-time components were linked to surface-proximal pore environments and microporous coating domains, whereas total porosity remained comparatively stable [15]. Electrical investigations further demonstrated that even clean, clay-poor Fontainebleau sandstone may exhibit measurable surface conductivity associated with the silica-water interface [16]. Earlier spectral induced polarization investigations on Fontainebleau additionally demonstrated strong sensitivity of the spectral response to cement style, pore geometry, and dual-porosity characteristics [21]. Together, these observations indicate that Fontainebleau sandstone should not be regarded as a purely surface-inert quartz framework, but rather as a quartz-rich rock whose petrophysical behavior may still be influenced by subtle silica-derived interfacial effects.

3.2 Investigated Fontainebleau Strata

To investigate the relationship between silica cementation style, pore structure, and petrophysical reproducibility, representative Fontainebleau samples from different stratigraphic and diagenetic domains were selected. The investigated material covers a transition from strongly cemented quartzitic strata to weakly cemented and highly porous sandstone intervals, thereby representing a natural progression of silica-cement evolution within the Fontainebleau Formation. This variability is particularly advantageous for CAL and SCAL investigations because it allows comparison between samples with similar bulk mineralogy but strongly different pore geometries, cement morphologies, and surface-controlled petrophysical properties.

Based on petrographic observations, µ-CT imaging, and SEM investigations, the investigated material was grouped into three representative fabric types (Fig. 3). Group A represents strongly cemented strata with extensive quartz cementation and low visible intergranular pore connectivity. The microstructure is dominated by tightly interlocked quartz grains and pervasive cement bridges, resulting in comparatively stiff and pore-throat-restricted fabrics. Group B represents porous sandstone with localized intergranular cementation, where quartz overgrowths and cement bridges coexist with still well-connected pore networks. This fabric type is particularly relevant because it combines preserved macroporosity with localized cement-related microporous domains and surface-active intergranular silica phases. Group C represents weakly cemented to non-cemented porous sandstone characterized by open intergranular pore networks, comparatively low cement abundance, and high visible pore connectivity.

The SEM and µ-CT observations illustrate that the Fontainebleau Formation cannot be regarded as a petrophysically uniform quartz reference material despite its high mineralogical purity. Instead, the investigated strata show pronounced heterogeneity in cement

distribution, pore-throat geometry, and microstructural organization. In particular, partially cemented domains frequently contain thin intergranular silica films and heterogeneous pore-lining cement textures that are difficult to identify using conventional bulk mineralogical methods alone. Such features are especially important because they may exert a disproportionate influence on interface-sensitive petrophysical measurements while contributing only minimally to total rock volume.

The investigated stratigraphic blocks therefore provide a suitable natural laboratory for evaluating the relationship between silica cement morphology and laboratory reproducibility. Strongly cemented samples primarily represent pore-throat reduction and quartz-framework stabilization, whereas partially cemented and weakly cemented samples preserve larger intergranular pore systems while still containing localized silica-derived interfacial domains. This distinction is particularly relevant for the interpretation of NMR and SIP measurements because both methods are highly sensitive to pore-surface interactions, surface relaxivity, electrical double-layer behavior, and microstructural heterogeneity.

The present study focuses primarily on the partially cemented and porous Fontainebleau strata because these samples exhibited the strongest variability during repeated saturation-measurement-drying cycles. Repetitive experiments revealed pronounced changes in NMR T_2 distributions and SIP phase responses despite stable bulk porosity and comparatively stable DC resistivity. The coexistence of preserved intergranular porosity and localized silica cementation therefore provides the most suitable conditions for investigating hydration-sensitive interfacial effects associated with amorphous or poorly ordered silica phases.

4 Methods and Lab-Protocol

For microstructural and petrophysical characterization, complementary imaging, pore-structure and transport-property analyses were performed on representative sub-samples of the investigated rock strata.

4.1 Methods

Air-dried sub-samples were examined by environmental scanning electron microscopy using an FEI Sirion D1625 ESEM operated under low-vacuum conditions at 0.6 mbar. The measurements were used for qualitative assessment of mineral phases, pore-lining features, and cement textures.

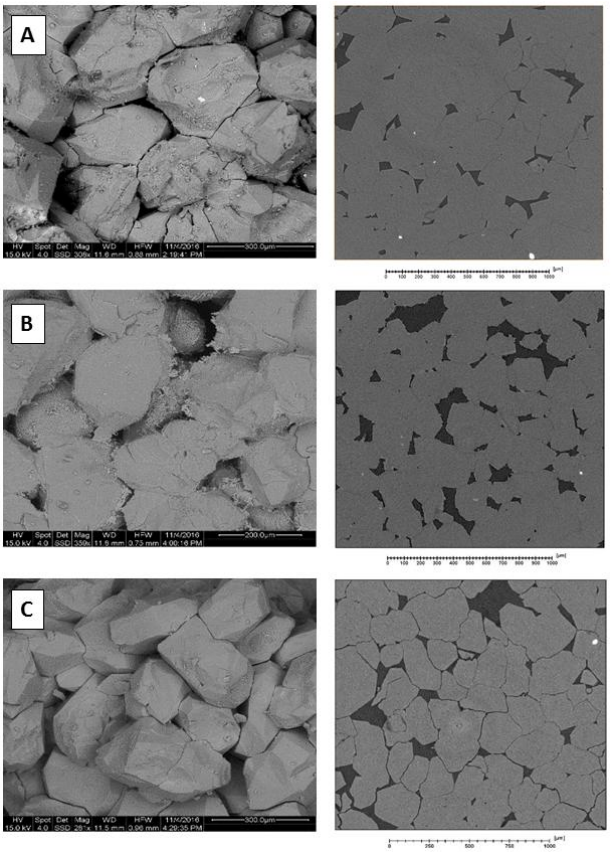

Figure 3: SEM (left) and µ-CT (right) images of representative samples from three different Fontainebleau stratigraphic blocks: A = strongly cemented strata, B = porous strata with intergranular cements, C = weakly cemented to non-cemented porous strata.

Three-dimensional pore-space characterization was performed by high-resolution X-ray micro-computed tomography using a Nanotom 180 M system (Waygate Technologies). Pore-throat characteristics were additionally investigated by mercury intrusion capillary pressure measurements using an AutoPore IV porosimeter (Micromeritics) over a pressure range from 0.003 to 400 MPa. Differential intrusion curves were evaluated to determine dominant pore-throat diameters.

Effective porosity was determined using the buoyancy method and complemented by nuclear magnetic resonance measurements, whereas gas permeability was measured under ambient conditions using a custom-built steady-state permeameter. Degassed NaCl solution with an electrical conductivity of approximately 20 mS/m was used as saturation fluid, corresponding to approximately 0.1 g/L NaCl depending on temperature and conductivity-to-TDS conversion.

Nuclear magnetic resonance measurements were performed with a Magritek Rock Core Analyzer operating at 2 MHz. Transverse relaxation-time distributions were used to characterize pore-size-related fluid responses and to derive NMR-based porosity from the total signal amplitude of the saturated samples. A standard Carr-Purcell-Meiboom-Gill (CPMG) pulse sequence was applied using an echo spacing of 0.1 ms, 30,000 echoes, a

recycle delay of 7.5 s, and 32 scans per measurement. T_2 distributions were obtained by inverse Laplace transformation using the standard Magritek inversion algorithm with automatic regularization. Identical acquisition and inversion parameters were used for all measurements before and after alkaline leaching.

Spectral induced polarization measurements were conducted with a SIP-Quad device (Radic Research) using a custom-built four-electrode core holder [21] over a frequency range from 1 mHz to 1 kHz. In addition to SIP phase and imaginary conductivity, direct-current resistivity was determined from the low-frequency conductivity response. All petrophysical measurements followed the laboratory protocols described in [22].

4.2 Alkaline Leaching

To evaluate whether poorly ordered or amorphous silica phases contribute to the observed petrophysical variability, selected split samples were subjected to controlled weak alkaline leaching. The treatment was designed as a selective extraction procedure intended to preferentially dissolve metastable silica phases while minimizing alteration of the crystalline quartz framework. Because amorphous silica is structurally less ordered, more hydrated, and chemically more reactive than crystalline quartz, it dissolves considerably faster under weak alkaline conditions [5].

The basic principle of the method relies on the increased solubility of amorphous silica in alkaline carbonate solutions. Dissolved Na_2CO_3 increases the concentration of hydroxyl-bearing species in the fluid, promoting hydrolysis of reactive siloxane bonds at the silica surface. Under these conditions, poorly polymerized or hydrated silica phases progressively dissolve into solution as dissolved silicic species, whereas the more stable quartz framework reacts much more slowly [5]. The selectivity of the procedure is therefore primarily kinetic rather than absolute: short and carefully controlled extraction preferentially removes reactive amorphous silica fractions, while prolonged exposure may increasingly affect microcrystalline or detrital quartz.

The leaching procedure was based on weak alkaline extraction using 1 wt.% Na_2CO_3 solution at approximately 85 °C for 4 hours, following established approaches for amorphous silica dissolution and extraction [5]. For the present study, the protocol was conservatively adapted for consolidated sandstone material. Leaching was therefore performed only on replicate material or sacrificial split samples and was always combined with pre- and post-treatment petrophysical and microstructural characterization.

Samples were conditioned to a defined initial state, immersed in pre-heated Na_2CO_3 solution under controlled laboratory conditions, and subsequently rinsed repeatedly with deionized water until low conductivity and near-neutral pH were reached. After reconditioning, the same petrophysical measurements were repeated in order to evaluate treatment-induced changes in pore structure, relaxation behavior, and electrical polarization response.

The procedure was not intended as a routine cleaning protocol, but rather as an operational tool to test whether hydration-sensitive amorphous silica phases contribute to non-reproducible NMR and SIP behavior.

4.3 Applied Lab-Protocol

For each investigated sample, a cylindrical core plug of approximately 50 mm length and 30 mm diameter was prepared. Prior to treatment, both end sections of the plug, each approximately 10 mm thick, were cut off and used as companion sub-samples for mineralogical, microstructural and pore-throat characterization. These end caps were assigned to SEM, µ-CT and MICP analyses, allowing the assessment of mineral phases, pore-space geometry and dominant pore-throat diameters before and after leaching. The remaining central core section was retained as the main plug for repeatable petrophysical measurements.

The main core plug was first characterized in its untreated state by determining mass, effective or connected porosity, gas permeability where applicable, NMR T_2 relaxation-time distributions, SIP phase response, imaginary conductivity and DC resistivity. Subsequently, the sample was subjected to the leaching procedure under controlled laboratory conditions. After leaching, the same petrophysical measurements were repeated on the identical main core plug in order to directly quantify treatment-induced changes in storage and transport properties. In parallel, the companion end-cap material was analyzed again, or compared with equivalent pre-treatment material, to relate changes in porosity, permeability, NMR response and electrical polarization behavior to mineralogical alteration, cement removal and modification of the pore-throat system.

This workflow enables a direct before-and-after comparison on the same main core plug while preserving dedicated material for destructive or partially destructive analytical methods. By combining repeated petrophysical measurements with SEM, µ-CT and MICP observations from the associated end caps, the approach links changes in bulk rock properties to microstructural and mineralogical modifications caused by the leaching treatment.

5 Results

This section presents the combined microstructural and petrophysical results obtained from MICP, porosity-permeability measurements, NMR, and SIP investigations before and after weak alkaline leaching. Particular focus is placed on changes in pore-throat structure, transport properties, relaxation behavior, and electrical polarization response across the different Fontainebleau strata in order to evaluate the influence of hydration-sensitive silica phases on petrophysical reproducibility.

5.1 Porosity & Permeability

The tight, strongly cemented strata (A) exhibited the most pronounced changes after leaching. Average porosity increased from 8.4% to 9.7%, corresponding to a relative increase of approximately 15.5%. In parallel, gas permeability increased from 0.1 mD to 21 mD. The intermediate strata (B) showed more moderate but still measurable changes. Average porosity increased from 11.5% to 12.2%, corresponding to a relative increase of approximately 6.1%, while permeability increased from 87 mD to 101 mD. In contrast, the porous strata (C) remained essentially unchanged after treatment. Average porosity changed only marginally from 18.2% to 18.25%, while permeability remained stable at approximately 312 mD.

Overall, the observed changes decrease systematically from the strongly cemented to the weakly cemented strata. Average porosity and Klinkenberg-corrected gas permeability values for the investigated Fontainebleau strata before and after weak alkaline leaching are summarized in Table 2. Reported values represent arithmetic mean values of five representative samples for each stratigraphic group (A–C).

Table 2: Porosity and Klinkenberg-corrected gas permeability of representative Fontainebleau strata before and after weak alkaline leaching. The tight and intermediate strata show measurable increases in porosity and permeability after treatment, whereas the porous strata remain essentially unchanged. The strongest relative permeability increase occurs in the tight cemented sample A, indicating that reactive silica phases primarily affected pore-throat-restricting cement domains.

Strata	A	B	C
Fabric type	Tight / cemented	Intermeadiate	Porous
Porosity before leaching [%]	8.40	11.50	18.20
Porosity after leaching [%]	9.70	12.20	18.25
Δ porosity [%]	+15.5	+6.1	+0.3
Permeability before leaching [mD]	0.1	87	312
Permeability after leaching [mD]	21	101	312
Δ permeability [%]	20,900	+16.1	0

5.2 MICP

The investigated Fontainebleau strata exhibit systematic differences in pore-throat distribution and intrusion behavior consistent with their observed cementation states (Fig. 4). The strongly cemented sample (A) shows a comparatively broad and heterogeneous pore-throat distribution with dominant intrusion contributions in the low- to intermediate-micrometer range and an extended intrusion tail toward smaller pore-throat diameters. The cumulative intrusion curve indicates progressive pore accessibility over a broad pressure range, consistent with a tight and partially restricted pore network.

In contrast, the intermediate sample (B) is characterized by a more distinct and narrower dominant pore-throat population centered in the intermediate micrometer range. Minor secondary intrusion features at smaller pore-throat diameters suggest the presence of additional microporous or partially cemented pore domains. Compared to sample A, the cumulative intrusion curve indicates a better connected and less restricted pore system.

The porous sample (C) exhibits a very sharp and dominant intrusion peak at comparatively large pore-throat diameters with only minor contributions from smaller pore classes. The cumulative intrusion behavior indicates rapid mercury access into a well-connected and comparatively homogeneous intergranular pore network. This sample therefore represents the least cemented and most pore-throat-dominated fabric of the investigated Fontainebleau strata. Conclusively, the MICP results demonstrate a progressive transition from heterogeneous, partially restricted pore systems in the cemented strata toward increasingly homogeneous and well-connected intergranular pore networks in the porous strata. The intermediate sample retains evidence of localized smaller pore-throat domains, which may be associated with intergranular cementation and pore-lining silica phases.

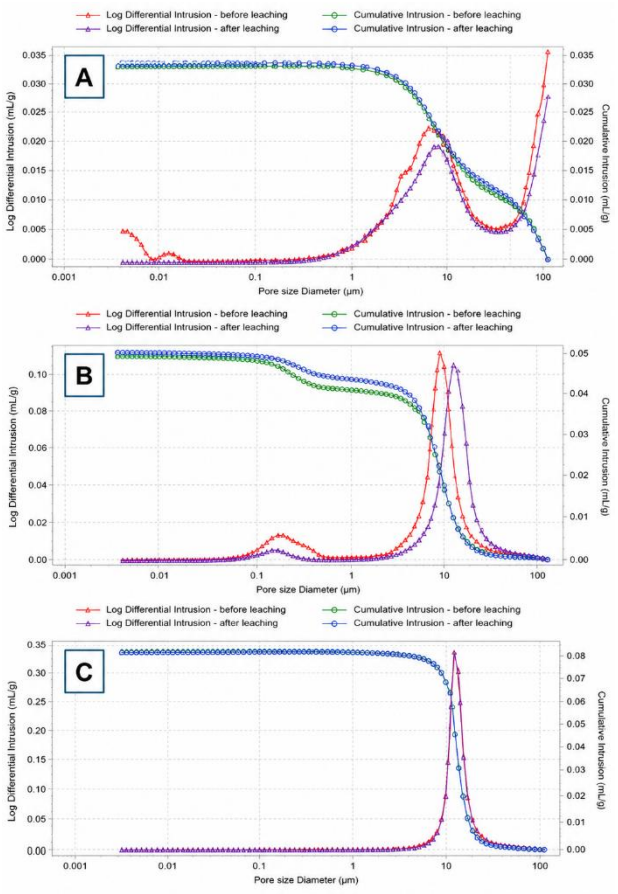

Figure 4: Mercury intrusion capillary pressure (MICP) results for representative Fontainebleau strata before and after weak alkaline leaching. Red/green curves represent the untreated state, whereas purple/blue curves show the post-leaching response. Left axis: log differential intrusion; right axis: cumulative intrusion. A = cemented, B = intermediate, C = uncemented Fontainebleau strata.

5.3 NMR

The NMR T_2 distributions show systematic changes after weak alkaline leaching for all investigated Fontainebleau strata (Fig. 5). NMR-derived porosity values remained in good agreement with the gravimetrically determined effective porosity before and after alkaline leaching. The observed differences were below 1.2 porosity units for all investigated samples, indicating that the treatment modified the surface-related relaxation behavior rather than the bulk pore volume. Each NMR measurement was repeated 5 times under identical experimental conditions to evaluate measurement reproducibility. The presented spectra correspond to the averaged response, whereas reproducibility was assessed from the complete set of repeated measurements. The most pronounced changes occur at short relaxation times (< 30 ms). Prior to leaching, all samples exhibit distinct short-T_2 contributions of varying magnitude, interpreted as surface-dominated or microporous relaxation domains associated with intergranular silica coatings or hydrated amorphous silica phases. After leaching, these short relaxation-time populations are strongly reduced or nearly completely removed.

The intermediate strata (B) retain a well-defined and symmetric dominant relaxation peak after treatment, whereas the tight (A) and porous (C) strata show a pronounced transformation of the long-relaxation-time response toward a similarly peaked distribution. Before leaching, samples A and C exhibit broad long-T_2 tails with limited signal decay toward longer relaxation times. After treatment, both spectra evolve toward narrower peak-like distributions comparable to type B. Overall, the post-leaching spectra indicate a substantially more homogeneous relaxation behavior and reduced contribution of short-relaxation-time domains across all investigated strata.

Relaxation components extending beyond approximately 10 s are treated as qualitative indicators only. Because these components lie close to the relaxation regime of highly mobile, near-bulk water and exceed the most strongly constrained part of the CPMG decay, they may be affected by inverse-Laplace broadening, baseline uncertainty, and regularization rather than representing discrete pore classes. Furthermore, hydrated amorphous silica or gel-like silica surfaces may overprint the relaxation response by introducing surface-associated water and exchange-averaged relaxation behavior. For this reason, the discussion focuses on relative changes in the short- and intermediate-T_2 domains, where the distributions are more reliably constrained.

It should be emphasized that T_2 relaxation times do not exclusively reflect pore size but also depend on surface relaxivity and the physicochemical properties of the pore walls. Consequently, differences between the investigated Fontainebleau strata cannot be interpreted solely in terms of pore-size distributions.

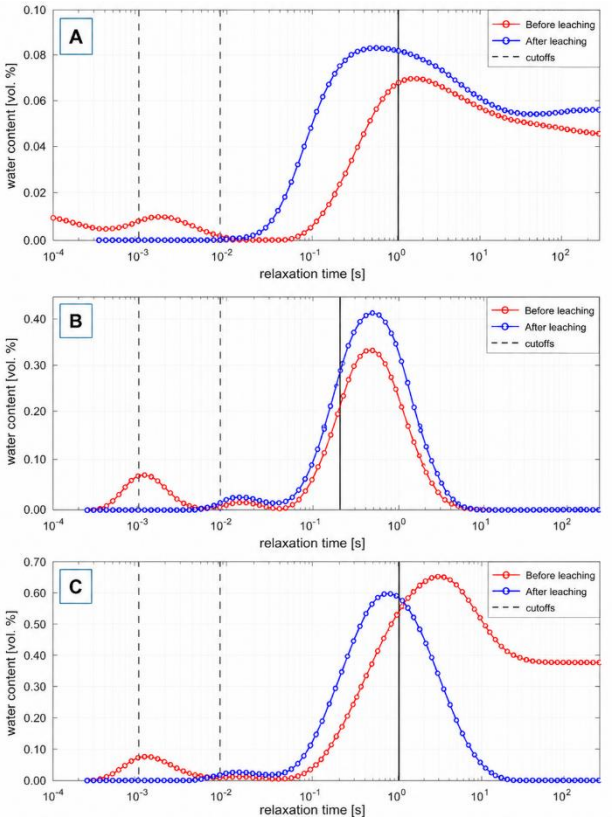

Figure 5: T_2 relaxation-time distributions of the Fontainebleau strata before (orange) and after (blue) weak alkaline leaching. Dashed vertical lines indicate relaxation-time cutoffs, the solid line T_{2mean} before leaching. (A) Tight, strongly cemented strata, (B) intermediate strata, and (C) porous strata. All samples show a strong reduction or near-complete disappearance of short-relaxation-time components after leaching.

5.4 SIP-Response

Repeated SIP measurements prior to alkaline leaching reveal pronounced reproducibility issues, particularly in the phase response (Fig. 6). In contrast, the specific electrical resistivity remains comparatively stable for all investigated Fontainebleau strata, showing only comparatively small deviations between repeated measurements. Mean specific resistivities remain within a narrow range for each stratigraphic group, with only minor variations between repeated saturation-drying cycles.

The strongest variability occurs in the phase spectra. The tight strata (A) exhibit substantial amplitude differences across repeated measurements over the entire investigated frequency range, with maximum deviations reaching approximately 25–30 mrad in the low- to intermediate-frequency range. At 1 mHz, the phase amplitudes of strata A varied between 6.5 and 24 mrad around an average value of 11 mrad, corresponding to asymmetric relative deviations of approximately −41 % to +118 %. The intermediate strata (B) show pronounced phase shifts and amplitude variations of approximately 5–10 mrad at low frequencies. At 1 mHz, phase amplitudes ranged from 9 to 19 mrad around an average value of 11.25 mrad, corresponding to relative deviations of approximately −20 %

to +69 %. In contrast, the porous strata (C) display smaller but still systematic phase offsets of approximately 0.5 mrad while largely preserving the overall spectral shape. At 1 mHz, these offsets correspond to approximately 0.5 ± 0.1 mrad, equivalent to about ±20 % relative to the mean value. For strata C, however, the observed phase offsets are close to the instrumental phase accuracy of approximately ±1 mrad and should therefore be interpreted cautiously.

After weak alkaline leaching, the variability of the phase response decreases strongly for all investigated strata. The post-leaching measurements cluster tightly within narrow reproducibility envelopes, typically remaining within approximately ± 2 – 3 mrad for all three fabric types. The improvement is particularly pronounced for the tight and intermediate strata, which previously exhibited the strongest non-reproducible behavior. Furthermore, the corresponding DC resistivity remained essentially unchanged after alkaline leaching, indicating that the treatment predominantly affected polarization processes rather than the bulk electrical conduction pathway.

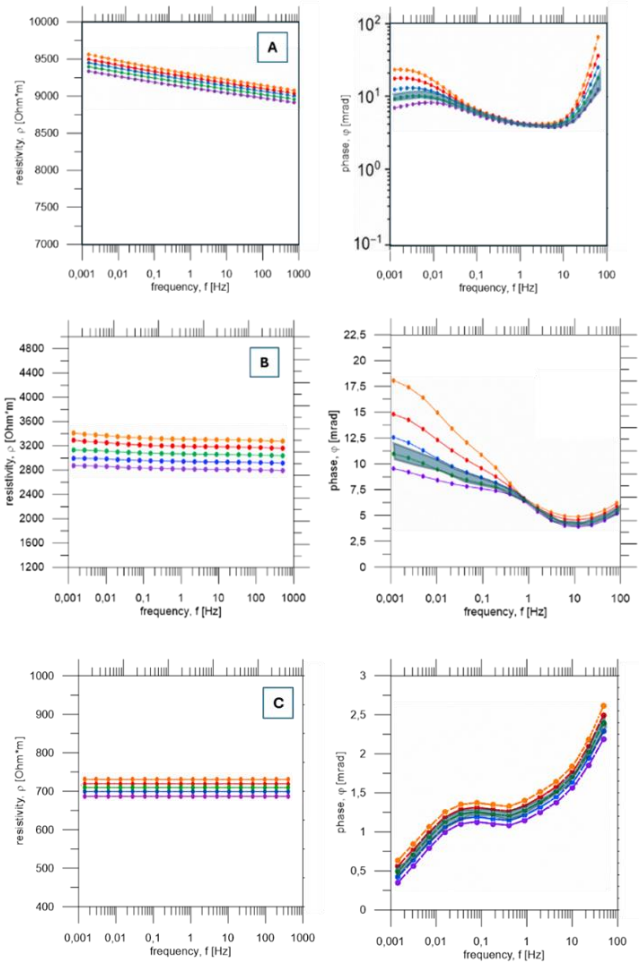

Figure 6: Resistivities and phase shift of the complex electric conductivity for the three investigated strata. Coloured lines indicate repeated measurements prior to leaching. The shadowed areas indicate the average phase response after leaching.

Overall, the SIP results demonstrate that the observed reproducibility issues primarily affect the polarization response rather than the bulk electrical resistivity. The strong stabilization of the phase spectra after leaching indicates that the non-reproducible behavior is linked to hydration-sensitive interfacial polarization processes associated with reactive silica-related surface domains.

6 Discussion & Conclusions

The present results demonstrate that hydration-sensitive amorphous silica is not merely a diagenetic curiosity but represents a previously overlooked source of systematic measurement variability in interface-sensitive petrophysical methods. Our study showcased that weak alkaline leaching affected the Fontainebleau samples on two coupled levels: the geometry of the pore-throat network and the physicochemical state of the pore surfaces. This distinction is essential for interpreting the results. Porosity, permeability and MICP describe how the accessible pore volume and pore-throat system changed, whereas NMR and SIP reveal how the fluid-filled pore space interacts with mineral surfaces. The central observation is that these two levels do not respond equally in all strata. The leaching effect is strongest in the cemented fabric, moderate in the intermediate fabric and weakest in the open porous fabric, but the stabilization of interface-sensitive NMR and SIP responses is observed across the investigated material. This indicates that the treated phase is not only a pore-blocking cement, but also an interface-active silica component.

The porosity-permeability and MICP results provide the geometrical framework for this interpretation. In the more strongly cemented samples, the leaching response is best understood as partial removal or weakening of silica cement at hydraulically critical pore throats. Even a small change in such locations can produce a disproportionately large permeability response, because flow is controlled by the narrowest and best-connected throats rather than by total pore volume alone. The corresponding MICP behavior supports this interpretation by showing that the cemented strata are characterized by heterogeneous and restricted pore-throat systems, whereas the less cemented strata exhibit more open and better-connected intergranular pore networks. Thus, Poro-Perm and MICP indicate that weak alkaline treatment partly opens or improves access to previously restricted pore-throat domains.

However, this geometrical explanation alone is not sufficient. If the leaching treatment only modified the connected pore network, the strongest changes would be expected in porosity, permeability and MICP-derived throat distributions, while NMR and SIP would largely follow those bulk pore-structure changes. Instead, the NMR and SIP responses show that a second process is involved: the reduction or stabilization of reactive pore-surface domains. The NMR spectra indicate that short relaxation-time contributions, which are commonly associated with high surface-to-volume ratios, microporous coating domains or enhanced surface

relaxivity, are strongly reduced after treatment. This is consistent with partial dissolution or chemical modification of poorly ordered, hydrated silica films or coating-related microporosity. The effect is therefore not only an increase in pore volume, but a change in the relaxation environment of the pore water.

The SIP response provides an independent confirmation of the same mechanism. The strongest reproducibility problem before leaching occurs in the phase response and imaginary conductivity, whereas DC resistivity remains comparatively stable. This pattern is characteristic of a process that affects interfacial polarization rather than bulk conduction. DC resistivity mainly reflects the connected brine-filled pore network, while SIP phase and imaginary conductivity are sensitive to electrical double-layer properties, surface charge, pore-throat polarization length scales and mineral-fluid interfacial chemistry. The post-leaching stabilization of the SIP spectra therefore indicates that the treatment reduced the contribution of a hydration-sensitive, polarizable silica surface phase. This agrees with the NMR interpretation and strengthens the conclusion that the controlling phase acts primarily at the pore-fluid interface.

Taken together, the four method groups define a coherent interpretation. Poro-Perm and MICP show where the treatment has a geometrical effect on pore accessibility and throat restriction. NMR and SIP show that the same treatment also suppresses unstable surface-controlled relaxation and polarization processes. The relative importance of these two effects depends on cementation state. In tightly cemented material, silica dissolution may affect both pore-throat connectivity and interfacial response. In intermediate material, both mechanisms are present but less extreme. In the most porous material, where porosity and permeability remain largely unchanged, the remaining NMR and SIP stabilization points more directly to an interface effect rather than to substantial pore-network alteration. This gradient from geometry-dominated to interface-dominated response is one of the strongest arguments that the leached phase is a subtle but petrophysically effective silica cement.

A direct microscopic verification of the leaching process by comparing identical pre- and post-treatment SEM surfaces was not feasible. SEM analysis requires destructive preparation of freshly fractured fragments, while the small fragments suitable for high-resolution imaging frequently disintegrated during alkaline treatment. Consequently, identical microstructural locations could not be re-examined after leaching. The interpretation presented here therefore relies on the internal consistency of the independent petrophysical observations (NMR and SIP), together with the SEM and electron microprobe evidence obtained prior to leaching. The systematic stabilization of both NMR and SIP responses following selective silica removal provides indirect but consistent evidence that the amorphous silica films represent the dominant source of the observed non-reproducibility.

This interpretation is consistent with the expected behavior of amorphous or poorly ordered silica in Na_2CO_3 solution. Weak alkaline leaching is not absolutely phase-selective; it is kinetically selective. Poorly ordered, hydrated and structurally reactive SiO_2 dissolves faster than crystalline quartz, so controlled treatment preferentially attacks the labile silica fraction. Prolonged exposure, however, may also affect microcrystalline quartz, syntaxial overgrowths or the detrital framework. The post-leaching state should therefore not be interpreted as a completely cleaned Fontainebleau sandstone, but as a partially modified state in which the contribution of the most reactive silica surfaces has been reduced.

This limitation is particularly important for Fontainebleau sandstone. The reactive silica phase appears to contribute not only to surface-controlled petrophysical behavior, but locally also to the cohesion of the pore framework. Attempts to continue the treatment until complete removal of the suspected phase would compromise sample integrity and may lead to disaggregation. Complete removal is therefore neither experimentally feasible nor conceptually desirable for CAL/SCAL interpretation. Once the rock fabric begins to fail, the experiment no longer isolates an accessory surface phase, but creates a different material. The relevant comparison is therefore not between natural Fontainebleau and an entirely silica-free end member, but between the untreated state and a controlled partially leached state in which the labile surface-active fraction has been reduced.

For CAL and SCAL workflows, the implication is that mineralogical purity and stable bulk properties do not guarantee petrophysical reproducibility. Quartz-rich reference sandstones may contain subtle amorphous or poorly ordered silica films that remain largely invisible to routine bulk mineralogy but affect measurements sensitive to mineral-fluid interfaces. Stable porosity or DC resistivity should therefore not be taken as evidence that the entire petrophysical response is stable. A combination of variable NMR T_2 distributions, variable SIP phase or imaginary conductivity and comparatively stable bulk properties should be treated as an indicator of a hidden surface-active phase.

Weak alkaline leaching can be useful in this context, but only as a diagnostic intervention on suitable material. It should not be regarded as a routine cleaning step before core analysis, because it changes the rock and may remove a diagenetic component that belongs to the natural pore system. Its value lies in testing causality: if reducing the labile silica fraction improves pore-throat accessibility and stabilizes interface-sensitive measurements, the phase can be identified as a source of systematic measurement bias.

Conclusively, the study demonstrates that amorphous or poorly ordered silica cement can act as an invisible bias in laboratory core analysis. It is invisible not because it cannot be imaged, but because its volumetric and bulk-mineralogical expression is small compared with its effect on pore-throat accessibility, pore-scale

relaxation and interfacial polarization. Fontainebleau sandstone remains a valuable reference material, but it is not necessarily petrophysically inert. Its use for benchmarking, inter-laboratory comparison and CAL/SCAL workflow validation should therefore include controlled conditioning, repeated measurements and, where possible, a combined interpretation of Poro-Perm, MICP, NMR and SIP rather than reliance on bulk mineralogy or single-method reproducibility alone.

The broader implication extends beyond Fontainebleau Sandstone itself. The present workflow demonstrates that repeated measurements, standardized conditioning and cross-method validation provide an effective strategy for identifying hidden sources of petrophysical non-reproducibility, even in apparently simple reference materials.

Acknowledgements

The authors would like to thank our reviewers, Elton Yang (Chevron) and Matthieu Mascle (IFPen) for improving the manuscript. Additionally, we thank Andre Marks (BGR, Hanover) for his support with the SEM imaging, and finally Stephan Kaufhold and Kristian Ufer for performing and discussing results from the leaching experiments.

References

[1] S.C. Haddad, R.H. Worden, D.J. Prior, P.C. Smalley, J. Sediment. Res. 76, 244–256 (2006)

[2] M. Thiry, B. Maréchal, J. Sediment. Res. 71, 473–483 (2001)

[3] R.H. Worden, M.W. French, E. Mariani, Geology 40, 179–182 (2012)

[4] M.W. French, R.H. Worden, Sediment. Geol. 284–285, 149–158 (2013)

[5] R.K. Iler, The Chemistry of Silica, Wiley, New York (1979)

[6] K.L. Page, T. Proffen, S.E. McLain, T.W. Darling, J.A. TenCate, Geophys. Res. Lett. 31, L24606 (2004)

[7] S. Akin, J.M. Schembre, S.K. Bhat, A.R. Kovscek, J. Pet. Sci. Eng. 25, 149–165 (2000)

[8] J.M. Schembre, A.R. Kovscek, Transp. Porous Media 65, 31–51 (2006)

[9] J.M. Schembre, G.-Q. Tang, A.R. Kovscek, SPE Reserv. Eval. Eng. 9, 239–250 (2006)

[10] B. Vega Martin, A.R. Kovscek, SPE ATCE, SPE-170918-MS (2014)

[11] I. Diabira, L.M. Castanier, A.R. Kovscek, SUPRI Technical Report 123 (2001)

[12] C.M. Ross, B. Vega Martin, J. Peng, M. Ikeda et al., SPE Western Regional Meeting, SPE-180369-MS (2016)

[13] B. Røgen, I.L. Fabricius, Pet. Geosci. 8, 287–293 (2002)

[14] S. Strand, M.L. Hjuler, R. Torsvik, J.I. Pedersen, M.V. Madland, T. Austad, Pet. Geosci. 13, 69–80 (2007)

[15] M.H. Jácomo, R.I.F. Trindade, M.W. French, E. Lucas-Oliveira, E.T. Montrazi, T.J. Bonagamba, AAPG Bull. 103, 2117–2137 (2019)

[16] A. Revil et al., Geophysics 79, D301–D318 (2014)

[17] C.T. Gomez, J. Dvorkin, T. Vanorio, Geophysics 75, E191–E204 (2010)

[18] M. Thiry, M. Bertrand-Ayrault, J.-C. Grisoni, Geol. Soc. Am. Bull. 100, 1283–1290 (1988)

[19] M. Thiry, A.R. Milnes, Bull. Soc. Géol. Fr. 195, 11 (2024)

[20] Y. Missenard, O. Parizot, J. Barbarand, Bull. Soc. Géol. Fr. 188, 28 (2017)

[21] M. Halisch et al., SCA2017-035 (2017)

[22] API RP40 (1998)